HOKKAIDO UNIVERSITY

Title	Tip artifact in atomic force microscopy observations of InAs quantum dots grown in Stranski-Krastanow mode
Author(s)	Shiramine, Ken-ichi; Muto, Shunichi
Description	Copyright © 2007 American Institute of Physics
Citation	Journal of Applied Physics, 101(033527) https://doi.org/10.1063/1.2434806
Issue Date	2007
Doc URL	https://hdl.handle.net/2115/17254
Type	journal article
File Information	JAP101-033527.pdf

Hokkaido University Collection of Scholarly and Academic Papers : HUSCAP

Tip artifact in atomic force microscopy observations of InAs quantum dots grown in Stranski–Krastanow mode

Ken-ichi Shiramine[a] and Shunichi Muto
Department of Applied Physics, Graduate School of Engineering, Hokkaido University, Sapporo 060-8628, Japan

Tamaki Shibayama, Norihito Sakaguchi, and Hideki Ichinose
Center for Advanced Research of Energy Conversion Materials, Hokkaido University, Sapporo 060-8628, Japan

Tamotsu Kozaki and Seichi Sato
Division of Energy and Environmental System, Graduate School of Engineering,Hokkaido University, Sapporo 060-8628, Japan

Yoshiaki Nakata[b] and Naoki Yokoyama
Fujitsu Laboratories, Ltd., Atsugi 243-0197, Japan

Masafumi Taniwaki
Department of Environmental Systems Engineering, Kochi University of Technology, Tosayamada, Kochi 782-8502, Japan

(Received 4 August 2006; accepted 4 December 2006; published online 13 February 2007)

The tip artifact in atomic force microscopy (AFM) observations of InAs islands was evaluated quantitatively. The islands were grown in the Stranski–Krastanow mode of molecular beam epitaxy. The width and height of the islands were determined using transmission electron microscopy (TEM) and AFM. The average $[\bar{1}10]$ in-plane width and height determined using TEM excluding native oxide were 22 and 7 nm, respectively; those determined using AFM including the oxide were 35 and 8 nm, respectively. The difference in width was due to the oxide and the tip artifact. The sizes including the oxide were deduced from TEM observations to be a width of 27 nm and a height of 6 nm with correction for the thickness of the oxide. The residual difference of 8 nm between the width determined using AFM and that determined using TEM including the oxide was ascribed to the tip artifact. The results enable us to determine the actual size of the islands from their AFM images. © *2007 American Institute of Physics*. [DOI: 10.1063/1.2434806]

I. INTRODUCTION

Quantum dots have been expected to produce novel optical and electronic devices because of their quantum size effect. Of the devices, quantum-dot lasers will be realized first.[1] Spintronic devices using quantum dots will bring innovations in areas including quantum information processing.[2]

Islands are grown in the Stranski–Krastanow (S–K) mode of molecular beam epitaxy (MBE).[3] The islands are quantum dots: they have a nanometer size and can confine carriers in them. The islands are suitable for devices since they are coherent and show intense photoluminescence. They are called self-assembled quantum dots.

The size of the islands is important information for realizing the application of the islands to devices. It is usually determined using transmission electron microscopy (TEM) and atomic force microscopy (AFM). TEM has the advantage that it leads directly to the actual size of the islands, although much time and effort are necessary to make samples sufficiently thin for electron transmission. On the other hand, AFM is a simple method that does not require sample preparation, although the size determined from an AFM image is not the actual size.

In AFM observations, it is widely known that the *tip artifact* prevents the determination of actual sizes[4–17] (Fig. 1). Because of the artifact, an AFM image does not represent the actual shape of an object but a nonlinear convolution of the shape of the object and the shape of the tip used. The in-plane width of the object is hence overestimated, while the height is determined correctly.[4–6,18] The artifact occurs because (i) the tip has a finite size, and (ii) a point of the tip other than its apex touches the surface.[5,7,8] The artifact is also called the convolution, dilation, or tip effect.

The tip artifact in AFM observations can be suppressed by (A) using a sharp tip or (B) the reconstruction of the actual shape from an image. To suppress the artifact, some research groups have attached a carbon-nanotube tip to a commercially available probe,[9,10] (A). Other groups have tried to reconstruct the actual shape of an object from its image by observing a sphere on a flat surface as a reference,[4–6,10–13] (B). A sphere is suitable as a reference for the following reason. If we have or know two of the following three things: an AFM image, the shape of the tip, and the shape of the object, we can obtain the remaining unknown.[14] We can hence reconstruct the actual shape of the object from

[a]Author to whom correspondence should be addressed; electronic mail: shira@eng.hokudai.ac.jp
[b]Present address: Nanoelectronics Collaborative Research Center, University of Tokyo, 4-6-1 Komaba, Meguro, Tokyo 153-8505, Japan.

 © 2007 American Institute of Physics

Downloaded 14 Feb 2007 to 133.87.26.100. Redistribution subject to AIP license or copyright, see http://jap.aip.org/jap/copyright.jsp

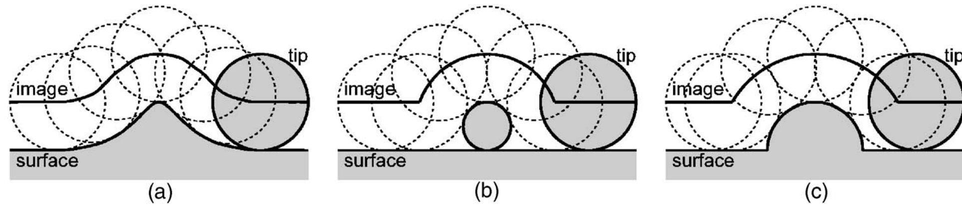

FIG. 1. Schematic views of AFM observations of (a) InAs S–K island, (b) sphere, and (c) hemisphere on flat surface. The AFM tip is depicted as a sphere having the same radius as the curvature radius of the tip. The tip artifact for the object having a steep surface, (b) and (c), causes a larger broadening than that for the object having a gentle surface, (a).

its AFM image if we know the size of the tip used. In addition, we can often determine the tip size by observing a sphere on a flat surface, because the height of the image is the diameter of the sphere and the width of the image is the sum of the diameter of the sphere and the diameter of the tip [Fig. 1(b)].

Geometric assumptions about an object produce an expression for broadening due to the AFM tip artifact. Assume that we observe a sphere of radius r using a tip of radius R [Fig. 1(b)]. Simple consideration yields $(R+r)^2=(w/2)^2+(R-r)^2$, where w is a broadened width of an image. It results in

$$w=4\sqrt{Rr}. \quad (1)$$

In a similar way, if we assume that an object is a hemisphere [Fig. 1(c)], $(R+r)^2=(w/2)^2+R^2$ leads to

$$w=2\sqrt{2Rr+r^2}. \quad (2)$$

A hemisphere is a more realistic model for the S–K islands than a sphere because of the hemispherelike shape of the islands.

In spite of much effort, only a few reports[4,10,12] have been published in which a tip artifact on the nanometer scale was evaluated. The artifact in observations of S–K islands has not yet been reported, although many authors have pointed out its presence.[18–23]

The determination of the broadening due to the tip artifact gives us a method by which we can extract the actual size of the S–K islands from their AFM images. The establishment of this method provides a practical way to determine the actual sizes of the islands of many samples. In fact, a research group that makes samples of the islands using MBE usually carries out hundreds of growth runs a year and observes all the samples using AFM, whereas it cannot do the same using TEM. This method using AFM, consequently, allows us to determine actual sizes of the islands of hundreds of samples a year.

In the application of the S–K islands to devices, the actual size of islands embedded in a cap layer is important. Note that the size of the embedded islands is different from that of uncapped islands because of surface segregation and interdiffusion. The relationship between the sizes of the two kinds of island is beyond the scope of the present study. Here, the relationship between the size of the uncapped islands determined using AFM and that determined using TEM is discussed as the first step.

In the present study, the size of the InAs S–K islands grown by MBE was determined using TEM and AFM. The size determined using TEM cannot be compared with that determined using AFM because native oxide was present between the epoxy and the crystalline (InAs and GaAs) in the TEM sample. Observations using TEM yielded the size excluding the oxide; observations using AFM yielded the size including the oxide. We hence carefully corrected the size determined using TEM for the thickness of the oxide to obtain a size which we can compare with that determined using AFM.

II. EXPERIMENTAL METHOD

Indium arsenide S–K islands were grown by MBE on a GaAs substrate at a low growth rate. A solid-source MBE with an As_4 beam was used. The (001) n^+GaAs substrate was fixed on a Mo block using In solder and was loaded into the MBE system. The native oxide on the substrate surface was desorbed by thermal etching. Then, a 250 nm GaAs buffer layer was grown at 610 °C at a rate of 0.21 μm/h. Next, InAs of 2.4 ML (monolayers) was grown at 500 °C at a rate of 0.006 ML/s. The temperature and As_4 pressure were maintained for 1.5 min after the growth, and then the electrical heating was turned off. No cap layer was grown. The uncalibrated V/III ratios were 60 for InAs and 63 for GaAs. A TEM sample and an AFM sample were cut from the same wafer.

We carried out (110) cross-sectional TEM observations. First, two pieces of the wafer were fixed face to face using epoxy. Then, a TEM sample was made from them by mechanical dimpling and Ar ion thinning (Gatan, model 600) at 4 kV and 15°. Field-emission TEM (JEOL, JEM-2010F) was performed at 200 kV. The width and height of the S–K islands were determined from the TEM images. The width was determined as the distance between the points where the profile rose from the baseline.

Observations using AFM were carried out in air with a MultiMode SPM/NanoScope IIIa (Veeco) operated in the contact mode. A probe (Veeco, NP-20), whose tip has a nominal curvature radius of 20 nm, made of Si_3N_4 was used. An image of 500×500 nm^2 size was obtained by the $[\bar{1}10]$ scan and was processed using IMAGEJ software.[24] Details of AFM observations and image processing are reported elsewhere.[25]

III. RESULTS AND DISCUSSION

A cross-sectional TEM lattice image of an InAs S–K island is shown in Fig. 2. An AFM image of InAs S–K islands is shown in Fig. 3. The surface density of the islands

Downloaded 14 Feb 2007 to 133.87.26.100. Redistribution subject to AIP license or copyright, see http://jap.aip.org/jap/copyright.jsp

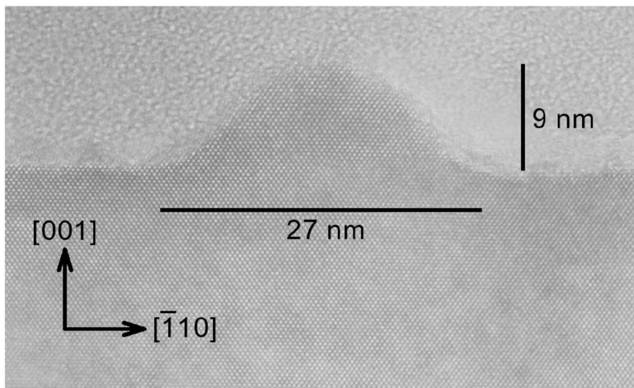

FIG. 2. Lattice image of InAs S–K island obtained by (110) cross-sectional TEM observation. The width and height of the island were determined to be 27 and 9 nm.

determined from the AFM images was 3.6×10^{10} cm^{-2}. The size of the islands was determined from the TEM and AFM images. Shown in Fig. 4 are the histograms of width and height determined by TEM observations of 171 islands and AFM observations of 267 islands. The average [$\bar{1}$10] in-plane width and height determined from the TEM images were 22 and 7 nm, respectively; those determined from the AFM images were 35 and 8 nm, respectively.

The results suggest that the width determined using AFM was 13 nm larger than that determined using TEM. This difference was due to the native oxide and the tip artifact. As will be shown, the size determined using TEM was corrected for the thickness of the oxide. The width determined using AFM was 8 nm larger than that corrected after being determined using TEM. The difference of 8 nm was ascribed to the tip artifact.

The size determined using TEM cannot be compared with that determined using AFM owing to the native oxide. The oxide on the surface was formed when the sample was removed from the MBE equipment into air. The oxide of the TEM sample was embedded in the epoxy (Sec. II). Observations using AFM yielded the island size including the oxide because AFM images represent a topography. Observations using TEM, on the other hand, yielded the island size excluding the oxide because a diffraction contrast forms TEM images. Indeed, since both were amorphous, the oxide could hardly be distinguished from the epoxy in TEM observations. For the above reasons, TEM observations could not yield the size of the islands including the oxide embedded in the epoxy.

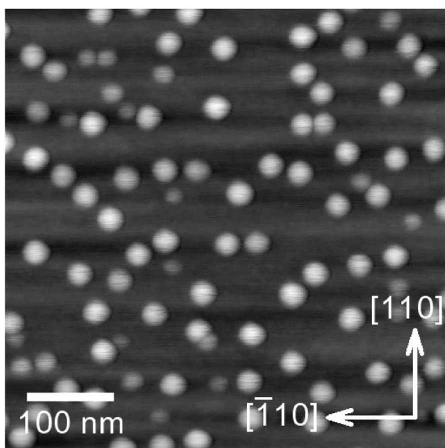

FIG. 3. AFM image of InAs S–K islands.

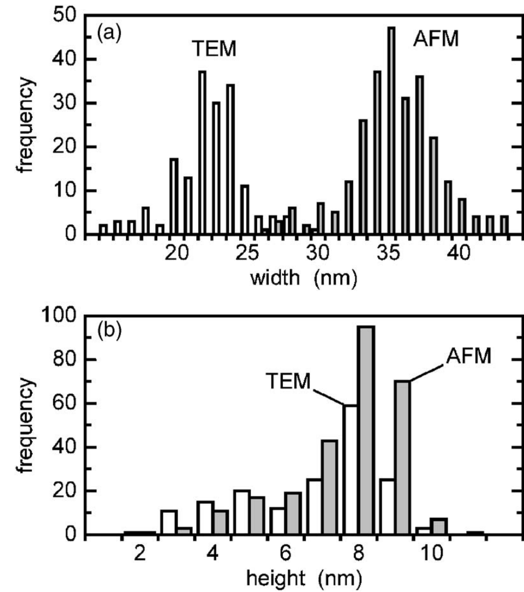

FIG. 4. Histograms of (a) [$\bar{1}$10] in-plane width and (b) height of InAs S–K islands obtained using TEM and AFM.

In spite of the above discussion, we succeeded in measuring the size of the islands including the native oxide using TEM in the course of the present study. In the TEM sample, there was a region where the epoxy peeled off the surface. This allowed us to determine the size including the oxide using TEM. The sizes of 51 islands in the region were measured at both (i) the surface of the oxide and (ii) the interface between the oxide and the InAs. The thickness of the oxide was 3 nm on a flat surface. The average [$\bar{1}$10] in-plane width and height determined in the former method, (i), were 28 and 6 nm, respecitvely; those determined in the latter method, (ii), were 23 and 7 nm, respectively (Table I). The latter sizes agreed with the above sizes determined by TEM observations of the 171 islands embedded in the epoxy. The width and height determined in the former method, (i), were 5 nm larger and 1 nm smaller than those determined in the latter method, (ii), respectively.

These differences between the sizes determined in both methods are reasonable because the difference between the

TABLE I. [$\bar{1}$10] in-plane width and height of the S–K islands determined using TEM and AFM at the interface (I) and surface (S). The number of the islands measured is shown in [ ], and the standard deviation is shown in ( ).

	TEM [51]		TEM [171]		AFM [267]
	I	S	I	S[a]	S
Width (nm)	23(2)	28(3)	22(3)	27	35(3)
Height (nm)	7(2)	6(2)	7(2)	6	8(1)

[a]The fourth column was calculated from the third column. 5 nm was added to the width, and 1 nm was subtracted from the height.

Downloaded 14 Feb 2007 to 133.87.26.100. Redistribution subject to AIP license or copyright, see http://jap.aip.org/jap/copyright.jsp

shape of the surface and that of the interface is understood as follows: The volume expands when the island surface is oxidized. The oxide on the top of an island is thinner than that on a flat surface because the surface area on the top is enlarged by expansion; in contrast, the oxide on the tail of an island is thicker than that on a flat surface because the surface area on the tail is reduced.

We corrected the previously described TEM observations of the width of 22 nm and the height of 7 nm for the thickness of the native oxide using the above difference of 5 nm in width and 1 nm in height to obtain a width of 27 nm and a height of 6 nm (Table I). The corrected sizes should be obtained if the surface of many islands were measured using TEM. They can hence be compared with the sizes determined using AFM. The width determined using AFM was, consequently, 8 nm larger than that corrected after being determined using TEM. The difference in height was 2 nm, and accordingly the heights determined by both methods were considered to agree.

The residual difference in width of 8 nm was ascribed to the tip artifact in AFM observations. The broadening of 8 nm is consistent with the nominal curvature radius, i.e., 20 nm, of the tip used. In fact, the artifact for the islands having a gentle surface causes a smaller broadening than the tip diameter (Fig. 1).

The broadening due to the tip artifact for the S–K islands grown at a standard rate of ~0.1 ML/s is similar to that for the islands grown at a low rate of 0.006 ML/s determined in the present study. For example, the islands grown at the standard rate have a diameter of approximately 10 nm (Fig. 2 of Ref. 25), and their AFM images show a diameter of approximately 20 nm (Fig. 4 of Ref. 25). This difference is also ascribed to the artifact.

The assumption that a S–K island has the shape of a hemisphere permits us to estimate an image width, which is consistent with that determined in the present study. In accordance with Eq. (2), if we observe a hemisphere whose radius r is 8 nm (Table I) using AFM with a tip whose radius R is 20 nm, we should obtain an image having a width w of 39 nm, which agrees with 35 nm (Table I) in the present results.

The broadening due to the tip artifact reported to date is different from that determined in the present study. There is, however, no inconsistency. Indeed, the difference in broadening can be understood in terms of the shape of objects, because the broadening depends on the shape of objects.

We can compare the results of AFM observations of a nanometer-sized sphere on a flat surface with those of the present study. Xu and Arnsdorf observed gold colloidal particles on mica using AFM and obtained an image with 11.7 nm height and 44.4 nm width.[4] Using Eq. (1), their results produce a tip radius R of 21 nm, which is close to that in the present study. Junno *et al.* observed GaAs particles using AFM to evaluate the artifact.[6] At first, they observed a particle whose image gave a width of 60 nm. Then, they moved the particle on a substrate by pushing it with the probe so that it made contact with another particle to obtain, from an image, a width of 90 nm for the two particles touching each other. Both actual diameter and the broadening were hence determined to be 30 nm. The above two results are consistent with our results, whereas the broadening reported is larger than ours, i.e., 8 nm. In fact, an object with a steeper surface induces a larger broadening owing to the artifact [Figs. 1(b) and 1(c)] than an object with a gentle surface [Fig. 1(a)]. Having a steeper surface, a sphere consequently induces a larger broadening than the islands. Next, Chen *et al.* observed gold nanoparticles using a tip made with a carbon nanotube to obtain, from an AFM image, a width of 10 nm.[10] The width of 10 nm was the sum of a nanoparticle diameter of 6 nm and a tip diameter of 3.5 nm; this is in accordance with Fig. 1(b). The small broadening is due to the small radius and a high aspect ratio of the tip.

Merz *et al.* reported AFM observations of CdSe S–K islands.[18] They extrapolated the relation between a height and a diameter of the islands to zero height to determine a broadening of 23 nm.

Using the broadening determined in the present study, we can determine the actual size of the S–K islands by correcting sizes obtained from AFM images. This is a practical way to determine the actual sizes of the islands of many samples, as discussed previously. The correction corresponds to a reconstruction of an actual shape, (B) in Sec. I. By the way, an AFM image depends on the size of the tip used: the employment of a probe of a different size leads to a different image for an identical object although the same type of probe is used. On the other hand, one should not use AFM if the exchange of a probe causes a complete change in an image. A probe having a large tip is, actually, excluded as a "bad probe" in observations.[4] For this exclusion, observations of an identical object result in almost the same image as long as the same type of probe is used. The dependence of images on tip size does not deteriorate the value of the correction using the artifact. Some groups have determined a tip size using a standard object;[12,26,27] this procedure allows us to confirm the tip size. Combination of the procedure and the correction using the broadening assures reliability of the correction.

In conclusion, the width of the InAs S–K islands determined using AFM was overestimated by 8 nm because of the tip artifact. The results enable us to determine the actual size of the islands from AFM observations. The results of AFM observations on the islands reported to date should be reevaluated considering the artifact.

[1] Y. Arakawa and H. Sakaki, Appl. Phys. Lett. **40**, 939 (1982).
[2] H. Ohno, Science **281**, 951 (1998).
[3] D. Leonard, M. Krishnamurthy, C. M. Reaves, S. P. Denbaars, and P. M. Petroff, Appl. Phys. Lett. **63**, 3203 (1993).
[4] S. Xu and M. F. Arnsdorf, J. Microsc. **173**, 199 (1994).
[5] P. Markiewicz and M. C. Goh, Langmuir **10**, 5 (1994).
[6] T. Junno, K. Deppert, L. Montelius, and L. Samuelson, Appl. Phys. Lett. **66**, 3627 (1995).
[7] U. D. Schwarz, H. Haefke, P. Reimann, and H.-J. Güntherodt, J. Microsc. **173**, 183 (1994).
[8] M. F. Tabet and F. K. Urban III, Thin Solid Films **290–291**, 312 (1996).
[9] K. I. Hohmura *et al.*, J. Electron Microsc. **49**, 415 (2000).
[10] L. Chen, C.-L. Cheung, P. D. Ashby, and C. M. Lieber, Nano Lett. **4**, 1725 (2004).
[11] J. Vesenska, R. Miller, and E. Henderson, Rev. Sci. Instrum. **65**, 2249 (1994).
[12] S. Xu and M. F. Arnsdorf, J. Microsc. **187**, 43 (1997).
[13] H. G. Abdelhady, S. Allen, S. J. Ebbens, C. Madden, N. Patel, C. J. Roberts, and J. Zhang, Nanotechnology **16**, 966 (2005).

Downloaded 14 Feb 2007 to 133.87.26.100. Redistribution subject to AIP license or copyright, see http://jap.aip.org/jap/copyright.jsp

[14]D. J. Keller and F. S. Franke, Surf. Sci. **294**, 409 (1993).
[15]L. Hellemans, K. Waeyaert, F. Hennau, L. Stockman, I. Heyvaert, and C. Van Haesendonck, J. Vac. Sci. Technol. B **9**, 1309 (1991).
[16]D. Keller, Surf. Sci. **253**, 353 (1991).
[17]P. Grütter, W. Zimmermann-Edling, and D. Brodbeck, Appl. Phys. Lett. **60**, 2741 (1992).
[18]J. L. Merz, S. Lee, and J. K. Furdyna, J. Cryst. Growth **184/185**, 228 (1998).
[19]S. Ruvimov *et al.*, Phys. Rev. B **51**, 14766 (1995).
[20]B. Junno, T. Junno, M. S. Miller, and L. Samuelson, Appl. Phys. Lett. **72**, 954 (1998).
[21]I. Mukhametzhanov, Z. Wei, R. Heitz, and A. Madhukar, Appl. Phys. Lett. **75**, 85 (1999).
[22]P. B. Joyce, T. J. Krzyzewski, G. R. Bell, T. S. Jones, S. Malik, D. Childs, and R. Murray, Phys. Rev. B **62**, 10891 (2000).
[23]Q. Xie, J. L. Brown, and J. E. Van Nostrand, Appl. Phys. Lett. **78**, 2491 (2001).
[24]URL: http://rsb.info.nih.gov/ij/
[25]K. Shiramine, S. Muto, T. Shibayama, H. Takahashi, T. Kozaki, S. Sato, Y. Nakata, and N. Yokoyama, J. Vac. Sci. Technol. B **21**, 2054 (2003).
[26]S. S. Wong, A. T. Woolley, T. W. Odom, J.-L. Huang, P. Kim, D. V. Vezenov, and C. M. Lieber, Appl. Phys. Lett. **73**, 3465 (1998).
[27]J. H. Hafner, C.-L. Cheung, T. H. Oosterkamp, and C. M. Lieber, J. Phys. Chem. B **105**, 743 (2001).

Downloaded 14 Feb 2007 to 133.87.26.100. Redistribution subject to AIP license or copyright, see http://jap.aip.org/jap/copyright.jsp